Spatial identification of nucleations in Superheated Droplet Detectors

M. Felizardo[1,2,3], R.C. Martins[3], T.A. Girard[1]

[1]*Centro de Física Nuclear, Universidade de Lisboa, 1649-003 Lisbon, Portugal*
[2]*Instituto Tecnológico e Nuclear, Estrada Nacional 10, 2686-953 Sacavém, Portugal*
[3]*Instituto de Telecomunicações, Av. Rovisco Pais 1, 1049-001 Lisboa, Portugal, 00 351 218418474, rcmartins@lx.it.pt*

Abstract — We present a new method for the identification of bubble nucleation in superheated droplet detectors. This is accomplished through some elaborate signal processing techniques applied to the acoustical recording of the nucleation events. These include the application of wavelets, chirp-z transform and pulse shape identification procedures to locate temporally and validate the nucleation together with back-propagation algorithms for spatial localization. Experimental results are given for the spatial localization at different temperatures and pressures.

I. Introduction

A superheated droplet detector (SDD) [1] is a generic denomination for a class of commonly employed systems for neutron detection [2]. SDDs have been used in neutron dosimetry for over a decade [3,4]; more recent applications include neutron spectrometry[5,6], and dark matter detection [7,8].
An SDD consists of a uniform dispersion of over-expanded, micrometric-sized halocarbon droplets suspended in a hydrogenated gel, each droplet of which functions as a mini-bubble chamber. Energy deposition by irradiation nucleates the phase transition of the superheated droplets, generating millimetric-sized bubbles [3] which can be recorded by either visual or chemical means. Because a bubble nucleation is accompanied by an acoustic shock wave, acoustic detection is also possible.
For several applications, the devices are operated under pressure, and submerged within a water bath which acts as both neutron moderator and temperature control. In tests with refrigerant-free modules, signals similar to bubble nucleation events were found to arise from pressure microleaks through the plastic SDD caps [9]. In rare event searches, these events may dominate the detector response, reducing the SDD application sensitivity by orders of magnitude. Improved construction has so far only succeeded in reducing the rate of these events.
Spatial localization of a nucleation through an array of microphones brings important information which serves several important purposes. One that might come up immediately to mind is the validation of a nucleation by automatically rejecting those that appear out of the vial volume. The detection of phantoms, i.e., replicas of a nucleation due to neighboring droplets also nucleating becomes easier since we now can correlate both time and space to identify them. Another, perhaps even more important, is that it allows for a nucleation spatial density mapping. From this spatial mapping of the nucleation important information related to the underlying physics might be inferred.

II. SDDs

A. Detector physics

The physics underlying the SDD operation is described in detail in [3]; we here provide only a short description. The superheated emulsions share the same working principle as bubble chambers, with the significant difference being that SDDs are continuously sensitive since the liquid is kept in steady-state superheated conditions (i.e., above its boiling point), whereas in the bubble chamber the liquid is only sensitized for brief periods of time. Two conditions are required [2] for the nucleation of the gas phase by energy deposition in the superheated liquid: (i) the energy deposited must be greater than a thermodynamic minimum, and (ii) this energy must be deposited within a minimum thermodynamic distance inside the droplet. The amount of energy and the critical size required for bubble nucleation depends on the composition and on the degree of superheat of the emulsion. Typically the higher the superheat of the droplets, the lower the nucleation energy required for their evaporation, i.e., the lower is the threshold energy of the detector. The threshold energy of each detector depends on the composition of the droplets, and their operating temperature and pressure.

B. Detector specification

SDDs are commonly fabricated with light halocarbons (freon) since, with a moderate superheat, they can be used in neutron detection inasmuch as they are only nucleated by energetic heavy ions such as those produced by fast neutrons [6]. If a high degree of superheat is applied, the nucleation can occur with sparsely ionising radiations such as photons and electrons [3].
Three types of SDDs are employed in our experimental trials: (i) "CCLF", implying a uniform dispersion of ~ 6 g of superheated droplets of CCl_2F_2 (R-12), and (ii) "CFI", implying a uniform dispersion of ~ 6 g of superheated droplets of CF_3I. Both of the detectors had their superheated droplets suspended in ~ 150ml of hydrogenated gel. (iii) A third "CCLF-m" and fourth "CCLF-M" detectors, implying the same uniform dispersion of ~ 6 g of superheated droplets of CCl_2F_2 (R-12), but modified with a different concentration in ~ 80ml of hydrogenated gel, "m" less ~ 60% and more "M" 60%.
All of these detectors were tested under pressure of 0, 1 and 2 atm.

III. Instrumentation for the SDD

A. Experimental setup and Spatial Identification

The acoustic shock wave associated with the rapid bubble expansion is accompanied by oscillating pressure pulses of <10 ms duration which can be acoustically recorded. The initial DAQ system, shown in Fig. 1 for just one channel, consists of five high quality electret microphone cartridges (MCE-200) with a frequency range of 20 Hz – 16 kHz (3 dB), SNR of 58 dB and a sensitivity of 7.9 mV/Pa at 1 kHz, associated to an electronic setup with high gain, low noise and high flexibility achieved through programmable gain, at the core of which stands a low-noise digitally controlled microphone preamplifier (PGA2500) which then couples to the input of an acquisition channel. Mechanically one of the microphones is inside the detector within a protective glycerine layer and the rest is around and beneath the detector, as shown in Fig.3. The electronic circuit with 5 microphones was assembled in a surface mount display, using a long shielded cable (~5 m) to connect the microphones to the pre-amplifiers; Fig. 2.

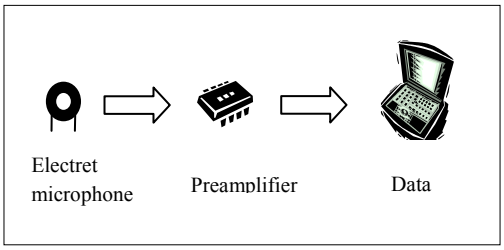

Fig. 1 Electronic set-up for data acquisition.

For the acquisition a National Instruments PXI-5105 high-speed digitizer was used, which is capable of acquiring up to 8 channels simultaneously at 60MSps. This gives a theoretical resolution of about 30μm considering an average sound speed, in the hydrogenated gel, of about $1800ms^{-1}$. This speed of sound was determined on a cylinder of hydrogenated gel 80cm long and with a 10cm radius. The measurements showed a speed of $1843ms^{-1}$ at 18ºC but without freon. We still have to access the dependence of the speed of sound with the freon and with temperature.
For the experimental validation the SDD was heated both globally using a heating bath and locally using very small platinum heating probes (2mm diameter head). The later setup was used to validate the localization algorithm.

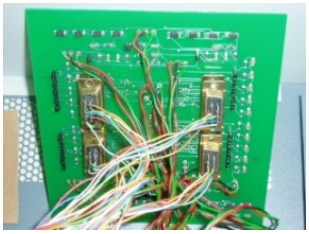

Fig. 2 Electronic circuit assembled in a surface mount display.

As mentioned before, to locate and correctly identify nucleations, discriminating spurious events, we used four microphones outside the vial and one inside. The spurious event suppression will hopefully be achieved by spatially-locating the bubble nucleation and correlating this information with the time interval of events, their relative phase information and time constant of each microphone.

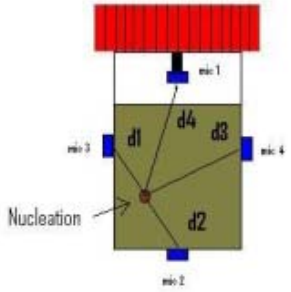

Fig.3 Position of the microphones around the detector vial.

In each of the five data vectors, corresponding to each of the five microphones, a relatively thorough approach is taken to identify each nucleation consisting of three steps. This starts with the use of a continuous wavelet Morlet based transform [11]. The choice of the base was the result of a maximum likelihood study between the typical nucleation and the several common wavelet bases using the crest factor as the cost function. The scales at which the transform is analysed depends on the gel, the pressure, temperature and whether the microphone is inside or outside the vial. For the results found in this paper the scales 17 and 33 were used.

From the output of the wavelet transform the selection of the possible candidates for nucleation is carried out by threshold analysis, being the threshold set at 5% of the crest factor. Each of the possible candidates for a nucleation will be analysed separately by centring a window on the location of the candidate, therefore segmenting the data. Each will endure a time and frequency analysis.

The time analysis consists in a simple pulse shape validation routine [12] in which each pulse is first amplitude demodulated and the time decay constant then determined through an exponential fit. The amplitude demodulation is achieved simply by taking the modulus of the Hilbert transform of the pulse waveform,

$$y(t) = \left| \mathrm{H}\{x(t)\} \right|,$$

as is depicted in Fig. 4, where the amplitude envelope, $y(t)$, is drawn in red.

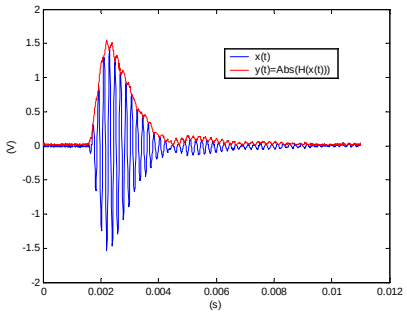

Fig. 4 Pulse shape of a bubble nucleation (blue line) and It's amplitude envelope (red line) as assessed by means of Eq. (1).

After the envelope has been obtained, the maximum and the minimum of the pulse shape are found to set the time window that will be used for evaluating the decaying time constant. The decaying part of the amplitude envelope is fit to an exponential,

$$h(t) = Ae^{\alpha t},$$

by means of a linear regression after linearization of the envelope,

$$\ln\left(y(t)\right) = \ln(A) + \alpha t + er(t),$$

where $er(t)$ corresponds to the residual of the fit. In Fig. 5 is shown both the decaying interval of the envelope and the exponential fit.

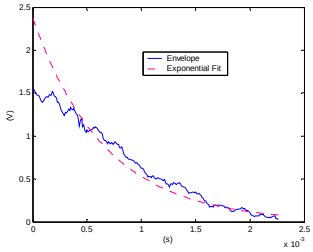

Fig. 5 Best fit of the exponential in Eq. (2) to the amplitude envelope of the pulse shown in Fig. 4 For this particular pulse the time constant was found to be 0.7 ms.

The frequency analysis is carried out for each candidate window using the Chirp-Z transform [13] to determine the spectrum between 200Hz and 700Hz, frequency window within which the oscillations of the nucleation are expected to be found.

Once all of the previously described three steps are taken all candidates that survived endure one final challenge: true nucleations must be present, nearly simultaneously, on all five channels.

Only those candidates that exist nearly simultaneously in all five channels will be located within the vial. The determination of each nucleation's position is an ill-posed inverse problem, being the direct problem the determination of the sound waves at each of the microphones knowing when, where and with what intensity did a nucleation occur.

The approach we have taken to solve this ill-posed inverse problem, since the geometry of the problem is well known, consists in mapping the vial volume with a regular, albeit dense, hexahedron mesh each with a volume of $5mm^3$. For each of these elements is determined the time differences of occurrence between each of the four external microphones to the one inside, taken as the reference. When a nucleation candidate is found the time differences between microphones is determined and a nearest neighbour algorithm is used to find the volume element which is the closest. It is obvious that this approach, as is now, cannot give any information on the intensity of the nucleation and is crude both in spatial resolution and in accuracy since in the forward problem we do not take into account the sound dispersion in the gel with a given bubble concentration, neither the reflections of the sound wave on the walls of the vial. Nevertheless, the experimental results, as we shall see in the next section are promising.

B. Experimental results

To validate the system we used a small heating probe (2mm diameter platinum heater) which was placed at known positions within the vial. Each time the probe was heated the location was estimated. From these measurements, at 0bar, 1bar and 2bar, and room temperatures from 15ºC to 20ºC we found the maximum error to be 1.2cm (accuracy) and the precision to be 1.8cm with 99.2% confidence. The errors where highest along the centre of the vial, especially in the middle, which proved to be good since no nucleations showed up "outside" the vial. The accuracy was better, < 9mm, at room temperatures of 18ºC, temperature at which the sound speed within the hydrogenated gel was measured, which might indicate high temperature dependence of the speed of sound in the medium.
We also heated the SDD in a bath and once again no "outside" nucleations were found which was in accordance with the knowledge that no leakage took place.

IV. Conclusions

The determination of the time constants of each nucleation is good to provide an in-depth knowledge of the gel media and is usually enough to discriminate real from fake nucleations. However, the spatial location of each nucleation serves three purposes:

1. to corroborate the data of the nucleation detection – fake events appear "outside" the vial.
2. to make easier the identification of a phantom.
3. to determine the spatial density of the nucleations and through it the incidence of the energy source.

In this paper we have shown an thorough approach to discriminate valid nucleations and to locate them within the vial. The spatial identification has clearly space for improvement, especially regarding a better model for sound propagation within the hydrogenated gel and glass reflections, temperature dependence of the sound speed and finer mesh resolution. It is also needed further validation of phantom suppression and a better understanding of spatial distribution of the nucleations.
Nevertheless, our experimental setup showed some encouraging results giving errors close to the mesh resolution.

Acknowledgments

This activity was financially supported by grants, POSI/EEA-ESE/60397/2004, POCTI/FIS/55930/2004, POCTI/FIS/57834/2004, POCTI/FNU/43683/2002 and POCTI/ESE/46995/2002 of the National Science Foundation of Portugal, co-financed by FEDER.

References

[1] R. E. Apfel. "The superheated drop detector". *Nucl. Instr.& Meth*. vol. 162. pp. 603-608. 1979.
[2] H. Ing.. H. C. Birnboim. "A bubble-damage polymer detector for neutrons". *Nucl. Tracks Radiat. Meas.*. vol. 8 (1-4). pp. 285-288. 1984.
[3] F. d'Errico. "Radiation dosimetry and spectrometry with superheated emulsions". *Nucl. Instr. & Meth*. vol. B184 (1-2). pp. 229-254. 2001.
[4] H. W. Bonin. G. R. Desnoyers and T. Cousins. "Fast neutron dosimetry and spectroscops using bubble detectors". *Radiat. Prot. Dosim.*. vol. 46 (4). pp. 265-271. 2001.
[5] F. d'Errico. W. G. Alberts. G. Curzio. S. Guldbakke. H. Kluge and M. Matzke. "Active neutron spectrometry with super heated drop detectors". *Radiat. Prot. Dosim.*. vol. 61(1-3). pp. 159-162. 1995.
[6] F. d'Errico. A. Prokofiev. A. Sanniko. H. Schuhmacher. "High energy neutron detection and spectrometry with superheated emulsions". *Nucl. Instr. & Meth*. vol. A505. pp. 50-53. 2003.
[7] F. Giuliani, TA Girard, G. Waysand, D. Limagne, T. Morlat, H.S. Miley, J.I. Collar, A.R. Ramos, M. da Costa, R.C. Martins, J.G. Marques, A.C. Fernandes. "Recent Results from the SIMPLE Dark Matter Search": arXiv: hep-ex/0504022.
[8] M. Barnabé-Heider, M. Di Marco, P. Doane et. al. "Improved Spin Dependent Limits from the PICASSO Dark Matter Search Experiment": arXiv hep-ex/0502028.
[9] J.I. Collar, J. Puibasset, TA Girard, D. Limagne, H.S. Miley and G. Waysand. "Prospects for SIMPLE 2000: a large-mass, low-background superheated droplet detectror for WIMP searches": New J. Phys. 2 (2000) 14.1.
[10] B213 (2004) 172-176 Nuclear Instruments and Methods in Physics Research
[11] B. B. Hubbard, *The World According to Wavelets: The story of a Mathematical Technique in the Making*, A. K. Peters, 1998.
[12] M. Felizardo et al, "Signal Discrimination in Superheated Droplet Detectors," Proceedings of the IMTC conference, Ottawa, 2004.
[13] L. R. Rabiner, B. Gold, *Theory and Application of Digital Signal Processing*, Englewood Cliffs, Prentice-Hall, pp. 393-399, 1975.
[14] F. Thomas, L. Ros, "Revisiting trilateration for robot localization," IEEE Transactions on Robotics, vol. 21, pp. 93-101, 2005.